

**Abstract**—An improved radiometric aging technique was used to examine annulus-derived age estimates from otoliths of the Atlantic tarpon, *Megalops atlanticus*. Whole otoliths from juvenile fish and otolith cores, representing the first 2 years of growth, from adult fish were used to determine  $^{210}\text{Pb}$  and  $^{226}\text{Ra}$  activity; six age groups consisting of pooled otoliths and nine individual otolith cores were aged. This unprecedented use of individual otolith cores to determine age was possible because of improvements made to the  $^{226}\text{Ra}$  determination technique. The disequilibria of  $^{210}\text{Pb}$ : $^{226}\text{Ra}$  for these samples were used to determine radiometric age. Annulus-derived age estimates did not agree closely with radiometric age determinations. In most cases, the precision ( $\text{CV} \leq 12\%$ ) among the otolith readings could not explain the differences. The greatest radiometric age was 78.0 yr for a 2045-mm-FL female, where the radiometric error encompassed the annulus-derived age estimate of 55 yr by about 4 yr. The greatest radiometric age for males was 41.0 yr for a 1588-mm-FL tarpon, where the radiometric error encompassed the annulus-derived age estimate of 32 yr by 1 yr. Radiometric age determinations in this study indicated that the interpretation of growth zones in Atlantic tarpon otoliths can be difficult, and in some cases may be inaccurate. This study provides conclusive evidence that the longevity of the Atlantic tarpon is greater than 30 years for males and greater than 50 years for females.

## Radiometric age validation of Atlantic tarpon, *Megalops atlanticus*

**Allen H. Andrews**

**Erica J. Burton**

**Kenneth H. Coale**

**Gregor M. Cailliet**

Moss Landing Marine Laboratories

8272 Moss Landing Road

Moss Landing, California 95039-9647

E-mail address (for A. H. Andrews): [andrews@mmlml.calstate.edu](mailto:andrews@mmlml.calstate.edu)

**Roy E. Crabtree**

National Marine Fisheries Service

9721 Executive Center Drive North

St. Petersburg, Florida 33702-2439

The Atlantic tarpon (*Megalops atlanticus*) is believed to be a long-lived fish. The strongest evidence is from a captive female Atlantic tarpon that lived to at least 63 years when it died in 1998 at the John G. Shedd Aquarium in Chicago, Illinois.<sup>1</sup> Life in the aquarium, however, is difficult to compare with life in the natural environment. A similar longevity of 55 years was estimated from growth zones in sagittal otoliths of a wild female tarpon (Crabtree et al., 1995). The annual periodicity of the growth zones used to estimate age was validated by using oxytetracycline up to an age of 9 yr in captive fish (Crabtree et al., 1995), but extrapolation of these results to older, wild fish, however, is fallible. In addition, wild Atlantic tarpon are highly migratory and inhabit waters that vary considerably in salinity (0 to 43 ppt) and temperature (17° to 37°C; Zale and Merrifield, 1989; Nichols<sup>2</sup>). It is uncertain what affect these changing conditions have on the formation of growth zones in the otoliths, but periods of stress have been shown to halt otolith growth (Campana, 1983). Furthermore, growth slows with age and growth zones become increasingly compressed, rendering otolith growth zones difficult to interpret. To circumvent the potential problems of otolith interpretation and to independently determine age, an application of the radiometric aging technique by using the  $^{210}\text{Pb}$ : $^{226}\text{Ra}$  disequilibria

in sagittal otolith cores (Campana et al., 1990) of Atlantic tarpon was performed, and the results are discussed in the context of existing estimated growth parameters.

### Materials and methods

Pooled and individual otolith cores from Atlantic tarpon were analyzed for  $^{210}\text{Pb}$  and  $^{226}\text{Ra}$  to determine age. Annulus-derived age estimates were based on six independent otolith readings determined by Crabtree et al. (1995) and resulted in a coefficient of variation of less than 12%. For radiometric age determination, otoliths were pooled into six groups based on annulus-derived age estimates, sex, and collection date. In addition, nine individual otoliths were analyzed. The age groups were selected to cover the full range of annulus-derived age estimates. Selected age groups had a narrow age range and members of the group were collected within a 6-month period. Otoliths of adult age groups were cored to the first two years of growth and otoliths of the youngest age groups

<sup>1</sup> Pamper, K. 1999. Personal commun. John G. Shedd Aquarium, 1200 S. Lakeshore Dr., Chicago, IL 60605.

<sup>2</sup> Nichols, K. M. 1994. Age and growth of juvenile tarpon, *Megalops atlanticus*, from Costa Rica, South Carolina and Venezuela. Senior thesis, Univ. South Carolina, Columbia, SC 29208, 52 p.

were analyzed whole because they were similar in size to cores from adult fish. Because 2-yr cores were large and the activity of  $^{226}\text{Ra}$  was relatively high (~10 to 100 times higher than usual; Andrews et al., 1999b), single otoliths were analyzed with the radiometric aging technique.

Coring the adult otoliths required establishing a target size and weight that closely approximated that of an otolith from a 2-year-old fish. Dimensions and weights of otoliths from four juvenile fish aged 2 years were recorded and averaged; the resultant dimensions were approximately 12 mm long by 6 mm high by 1 mm thick and a weight of 0.1 g. Each otolith from each adult age group was sculpted into this shape and weight by being hand-ground on a Buehler Ecomet® III lapping wheel. All samples were cleaned of any adhering contamination by following specific procedures described elsewhere (Andrews et al., 1999b). These clean samples were placed in acid-cleaned 100-mL Teflon® PFA Griffin beakers and dried at 85°C for 48 h.

A detailed protocol describing sample preparation, chromatographic separation of  $^{226}\text{Ra}$  from barium and calcium, and analysis of  $^{226}\text{Ra}$  using thermal ionization mass spectrometry (TIMS) is described elsewhere (Andrews et al., 1999b). Only an overview of the  $^{226}\text{Ra}$  procedures is given here with details on the determination of  $^{210}\text{Pb}$  activity. Because the levels of  $^{226}\text{Ra}$  and  $^{210}\text{Pb}$  typically found in otoliths were extremely low (from femtograms [ $10^{-15}$  g] for  $^{226}\text{Ra}$  and attograms [ $10^{-18}$  g] for  $^{210}\text{Pb}$ ) and because of the great potential for contamination from calcium, barium, and lead, trace-metal clean procedures and equipment were used throughout sample preparation, separation, and analysis. All acids used were double distilled (GFS Chemicals®) and dilutions were made with Milli-pore® filtered Milli-Q water (18 M $\Omega$ /cm).

To determine  $^{226}\text{Ra}$  activity with thermal ionization mass spectrometry (TIMS), the sample must be clean of naturally occurring organics (such as otolin). Organic residues elevate background counts in the  $^{226}\text{Ra}$  region and increase the analytical uncertainty during TIMS analysis. Dried and weighed samples were dissolved in beakers on hot plates at 90°C by adding 8N HNO<sub>3</sub> in 1–2 mL aliquots. Alternation between 8N HNO<sub>3</sub> and 6N HCl, with an aqua regia transition, several times resulted in complete sample dissolution. The dried sample, after dissolution, formed a yellowish foam. To further reduce any remaining organics, and to put the residue into the chloride form required for the  $^{210}\text{Pb}$  activity determination procedure, the samples were redissolved in 1 mL 6N HCl and taken to dryness five times at ~90°C. A whitish residue indicated that a sufficient amount of the organics had been removed. These samples were used to determine  $^{210}\text{Pb}$  activity prior to TIMS analysis.

### Determination of $^{210}\text{Pb}$ Activity

To determine  $^{210}\text{Pb}$  activity in the otolith samples, the alpha-decay of  $^{210}\text{Po}$  was used as a daughter proxy for  $^{210}\text{Pb}$ . To ensure that activity of  $^{210}\text{Po}$  was due solely to ingrowth from  $^{210}\text{Pb}$ , the time elapsed from capture to  $^{210}\text{Pb}$  determination was greater than 2 yr. Samples pre-

pared for  $^{210}\text{Po}$  analysis were spiked with  $^{208}\text{Po}$ , a yield tracer. The amount of  $^{208}\text{Po}$  added was estimated on the basis of observed  $^{226}\text{Ra}$  levels in otoliths of juvenile tarpon. This amount was adjusted to five times the expected  $^{210}\text{Po}$  activity in the otolith sample to reduce error in the  $^{210}\text{Pb}$  activity determination. The spiked samples were redissolved in approximately 50 mL of 0.5N HCl on a hot plate at 90°C covered with a watch glass. The  $^{210}\text{Po}$  and  $^{208}\text{Po}$ -tracer were autodeposited for 4 hours onto a silver planchet (Flynn, 1968). The activities of these isotopes were determined by using alpha-spectrometry on the plated samples. Quantification of the  $^{210}\text{Po}$  was made by subtracting a detector blank and reagent counts from each peak region-of-interest, by multiplying the  $^{210}\text{Po}$ : $^{208}\text{Po}$  count ratio by the known  $^{208}\text{Po}$  activity, and by correcting for decay back to the time of plating. To attain sufficient counts, samples were counted for 21–23 d. The solution remaining after polonium plating was dried and saved for  $^{226}\text{Ra}$  analyses.

### Determination of $^{226}\text{Ra}$ Activity

To prepare the samples for  $^{226}\text{Ra}$  activity determination with TIMS, each sample was spiked with  $^{228}\text{Ra}$ , a yield tracer, and a newly developed ion-exchange separation technique was used to isolate radium from calcium and barium (Andrews et al., 1999b). The final samples were processed by using TIMS and the measured ratios of  $^{226}\text{Ra}$ : $^{228}\text{Ra}$  were used to calculate  $^{226}\text{Ra}$  activity. The analysis of unspiked otolith samples indicated that  $^{228}\text{Ra}$  was not present in measurable quantities in otoliths of juvenile fish, and no adjustment was necessary for the measured  $^{226}\text{Ra}$ : $^{228}\text{Ra}$  ratio in spiked samples.

### Radiometric age determination

To assess the feasibility of applying the radiometric aging technique to Atlantic tarpon, uptake of  $^{210}\text{Pb}$  and  $^{226}\text{Ra}$  was assessed in otoliths from juvenile fish. Because the age of juvenile Atlantic tarpon is better constrained than that of adults, age was determined by using  $^{210}\text{Pb}$ : $^{226}\text{Ra}$  disequilibria in whole otoliths from juvenile fish. For the juvenile otolith samples, the age determined would be higher than expected if a significant amount of exogenous  $^{210}\text{Pb}$  was incorporated into the otolith.

Age was estimated from the measured  $^{210}\text{Pb}$  and  $^{226}\text{Ra}$  activities (Eqs. 1 and 2). Because the activities were measured from the same sample, the calculation was independent of sample mass. For adult samples, where estimated age was greater than that of the 2-year-old core, radiometric age was calculated as follows with an equation derived from Smith et al. (1991) to compensate for the ingrowth gradient of  $^{210}\text{Pb}$ : $^{226}\text{Ra}$  in the otolith core,

$$t_{\text{age}} = \frac{\ln \left( \frac{1 - \frac{A^{210}\text{Pb}_{tc}}{A^{226}\text{Ra}_{\text{TIMS}}}}{(1 - R_0) \left( \frac{1 - e^{-\lambda T}}{\lambda T} \right)} \right)}{-\lambda} + T, \quad (1)$$

where  $t_{age}$  = the radiometric age at the time of capture;  
 $A^{210}\text{Pb}_{tc}$  = the  $^{210}\text{Pb}$  activity corrected to time of capture;  
 $A^{226}\text{Ra}_{\text{TIMS}}$  = the  $^{226}\text{Ra}$  activity measured with TIMS;  
 $R_0$  = the activity ratio of  $^{210}\text{Pb}$ : $^{226}\text{Ra}$  initially incorporated;  
 $\lambda$  = the decay constant for  $^{210}\text{Pb}$  ( $\ln(2)/22.26$  yr);  
 and  
 $T$  = the core age (2 yr).

The radiometric age calculation for the juvenile age-group was determined by iteration of an equation derived from Smith et al. (1991),

$$\frac{A^{210}\text{Pb}_{tc}}{A^{226}\text{Ra}_{\text{TIMS}}} = 1 - (1 - R_0) \left( \frac{1 - e^{-\lambda t_{age}}}{\lambda t_{age}} \right), \quad (2)$$

where all equation components were as defined above. A radiometric age range, based on the analytical uncertainty, was calculated for each sample by applying the calculated error for  $^{210}\text{Pb}$  and  $^{226}\text{Ra}$  activity determinations to the measured  $^{210}\text{Pb}$ : $^{226}\text{Ra}$ . Calculated error included the standard sources of error (i.e. pipetting, spike, and calibration uncertainties), alpha-counting statistics for  $^{210}\text{Pb}$  (Wang et al., 1975), and an analysis routine used to run  $^{226}\text{Ra}$  samples on the thermal ionization mass spectrometer (Andrews et al., 1999b).

### Age estimate accuracy

To compare annulus-derived age with radiometric age, a plot of the annulus-derived age estimate and measured  $^{210}\text{Pb}$ : $^{226}\text{Ra}$  activity ratio was compared graphically to the expected  $^{210}\text{Pb}$ : $^{226}\text{Ra}$  activity ratio from ingrowth. This comparison included a graphical compensation for the  $^{210}\text{Pb}$ : $^{226}\text{Ra}$  gradient in the core sample. This model assumed a linear mass-growth rate for the first two years of growth. Annulus-derived age range and the analytical uncertainty of the activity ratio were plotted with each data point. A direct comparison of annulus-derived age and radiometric age was made in a plot where a regression of the data was compared to a line of agreement or slope of one. A paired two-sample  $t$ -test was used to determine if a significant difference existed between the age estimates.

Von Bertalanffy growth functions were fitted to the radiometric ages with FISHPARM software (Saila et al., 1988) and plotted with the annulus-derived ages and growth functions from Crabtree et al. (1995) for a visual comparison. High and low radiometric age and the size range of each sample were plotted for each data point. No statistical comparison was made between the growth functions because of the low number of samples and wide confidence interval for each parameter.

## Results

Six age groups and nine individual otolith cores were selected for radiometric analyses (Table 1). Of the age group

samples, three male samples and three female samples were selected to span the estimated age range of each sex. Male age groups were 2–4 yr, 18–21 yr, and 31–36 yr. Female age groups were 3–4 yr, 15–24 yr, and 48–50 yr. For each age group the capture dates were within a 6-month period, except the 2–4 yr male age group where the period spanned 7 months. Individual otolith core samples ranged in annulus-derived age from 13 yr to 32 yr for males and 35 yr to 55 yr for females. The greatest annulus-derived ages were for females; the oldest female was estimated to be 55 yr and the oldest male was 36 yr. Fork length was lowest for the juvenile age groups and did not overlap with older age groups. There was some overlap between the middle and old age groups. Males were typically smaller than females; the largest male was 1620 mm FL and the largest female was 2045 mm FL. The number of otoliths used in each age group ranged from 4 to 11 with the fine-cleaned sample weight ranging from 0.3314 to 1.0718 g. The individual core samples ranged in weight from 0.0884 g to 0.1366 g. These samples are the lowest weights and the first individual otolith cores ever used for radiometric age determination.

Activities of  $^{210}\text{Pb}$  and  $^{226}\text{Ra}$  were determined and combined to form an activity ratio for each sample (Table 2). The  $^{210}\text{Pb}$  activity spanned a wide range and increased from juveniles to adults by as much as 88 times. The lowest activities were for the juvenile samples (0.003 and 0.005 disintegrations per gram [dpm/g]) and the highest activity was 0.265 dpm/g ( $\pm 6.0\%$ ) for the largest male (1620 mm FL). The activity of  $^{226}\text{Ra}$  varied by an order of magnitude and ranged from 0.044 dpm/g ( $\pm 1.53\%$ ) to 0.401 dpm/g ( $\pm 1.02\%$ ). Calculated  $^{210}\text{Pb}$ : $^{226}\text{Ra}$  ranged, as predicted, between 0 and 1; the lowest activity ratios were for the juvenile samples and the highest were for large adults. All low and high ratios were within the limits of 0 to 1 (values  $>1$  are mathematically undefined; Eqs. 1 and 2) except for the largest female (2045 mm FL), which had an upper limit that exceeded 1. Radiometric age of the juvenile samples was very close to the expected age (Table 3). Exogenous  $^{210}\text{Pb}$  was, therefore, either not present or present in negligible quantities. This was inferred to be true for the core, or juvenile region, of adult Atlantic tarpon otoliths.

Comparison of annulus-derived ages and radiometric ages indicated there were differences in the aging results for each technique (Table 3). In most cases, the precision among the otolith readings could not explain the differences. In four cases, the different age estimates overlapped, but the extent of overlap was at the extreme of the age range. The lowest radiometric ages were one year for the samples from juvenile fish and the highest was 78.0 yr for the largest adult female.

A graphical comparison of the expected  $^{210}\text{Pb}$ : $^{226}\text{Ra}$  disequilibria from ingrowth with the measured  $^{210}\text{Pb}$ : $^{226}\text{Ra}$  indicated there was variation in the measured results above and below what was expected (Fig. 1). The low radiometric age for the juvenile age-groups indicated that uptake of exogenous  $^{210}\text{Pb}$  ( $R_0$ ; Campana et al., 1990) by juveniles was insignificant. Therefore, the best model for ingrowth of  $^{210}\text{Pb}$  from  $^{226}\text{Ra}$  in tarpon otoliths was for  $R_0 = 0.0$ .

**Table 1**

Detailed summary of data for pooled otolith age groups and single otoliths from *Megalops atlanticus*. Age range of age groups is based on annulus-derived age estimates. Capture dates and average fork length are listed for comparison. Age groups consisted of 4 to 11 otolith cores and amounted to ~1 g. Single otolith cores weighed close to 0.1 g.

Age-group or single otolith age (yr)	Capture date or range	Fork length (mm $\pm$ SD)	Number of otoliths	Sample weight (g)
<b>Male</b>				
2-4 <sup>1</sup>	7 Mar-16 Oct 1989	568 $\pm$ 80	7	0.6786
13	22 Jun 1989	1499	1	0.1129
17	4 Jul 1989	1452	1	0.1124
18-21	1 May-25 Jul 1989	1442 $\pm$ 78	10	1.0498
31-36	12 Jun-7 Jul 1990	1532 $\pm$ 73	4	0.3480
32	6 Jun 1989	1588	1	0.1279
32	19 Jul 1992	1620	1	0.1220
<b>Female</b>				
3-4 <sup>1</sup>	24 Jan-15 Jul 1989	583 $\pm$ 59	9	0.8775
15-24 <sup>2</sup>	6 Jun-12 Aug 1989	1641 $\pm$ 92	11	1.0718
35	4 Jul 1989	1613	1	0.1002
36	12 May 1992	1780	1	0.1331
37	12 Jun 1993	1950	1	0.1167
44	2 Sep 1991	2040	1	0.1366
48-50	20 Apr-20 Jun 1989	1708 $\pm$ 110	4	0.3314
55	4 Mar 1991	2045	1	0.0884

<sup>1</sup> Whole juvenile otoliths.

<sup>2</sup> Ten otoliths ranging in age from 21 to 24 yr; one 15-yr-old otolith was erroneously included in this age group.

**Table 2**

Radiometric results for each *Megalops atlanticus* age group and single otolith samples. Activities are expressed as disintegrations per minute per gram (dpm/g).

Age-group or single otolith age (yr)	Sample weight (g)	<sup>210</sup> Pb (dpm/g) $\pm$ % error <sup>1</sup>	<sup>226</sup> Ra (dpm/g) $\pm$ % error <sup>2</sup>	<sup>210</sup> Pb: <sup>226</sup> Ra activity ratio	<sup>210</sup> Pb: <sup>226</sup> Ra low	<sup>210</sup> Pb: <sup>226</sup> Ra high
2-4 <sup>3</sup>	0.6786	0.005 $\pm$ 6.7	0.258 $\pm$ 1.03	0.017	0.016	0.019
13	0.1129	0.043 $\pm$ 12.1	0.085 $\pm$ 1.52	0.507	0.439	0.577
17	0.1124	0.035 $\pm$ 13.6	0.061 $\pm$ 1.61	0.568	0.483	0.656
18-21	1.0498	0.072 $\pm$ 3.4	0.246 $\pm$ 1.01	0.292	0.280	0.305
31-36	0.3480	0.094 $\pm$ 5.3	0.181 $\pm$ 1.25	0.520	0.486	0.555
32	0.1279	0.031 $\pm$ 13.5	0.044 $\pm$ 1.53	0.712	0.607	0.821
32	0.1220	0.265 $\pm$ 6.0	0.401 $\pm$ 1.02	0.663	0.617	0.710
<b>Female</b>						
3-4 <sup>3</sup>	0.8775	0.003 $\pm$ 5.7	0.217 $\pm$ 1.06	0.015	0.014	0.016
15-24	1.0718	0.059 $\pm$ 3.9	0.163 $\pm$ 1.07	0.362	0.345	0.381
35	0.1002	0.119 $\pm$ 8.2	0.299 $\pm$ 1.35	0.397	0.360	0.435
36	0.1331	0.086 $\pm$ 8.5	0.144 $\pm$ 2.24	0.597	0.534	0.663
37	0.1167	0.126 $\pm$ 8.0	0.243 $\pm$ 1.18	0.518	0.471	0.567
44	0.1366	0.113 $\pm$ 7.4	0.170 $\pm$ 1.33	0.667	0.609	0.726
48-50	0.3314	0.148 $\pm$ 4.5	0.266 $\pm$ 1.19	0.555	0.524	0.587
55	0.0884	0.086 $\pm$ 12.2	0.094 $\pm$ 1.42	0.909	0.787	1.035

<sup>1</sup> Calculation based on standard deviation of <sup>210</sup>Pb activity; Wang et al., 1975.

<sup>2</sup> Calculation based on TIMS analysis routine ( $\pm$ 1 SE).

<sup>3</sup> Whole juvenile otoliths.

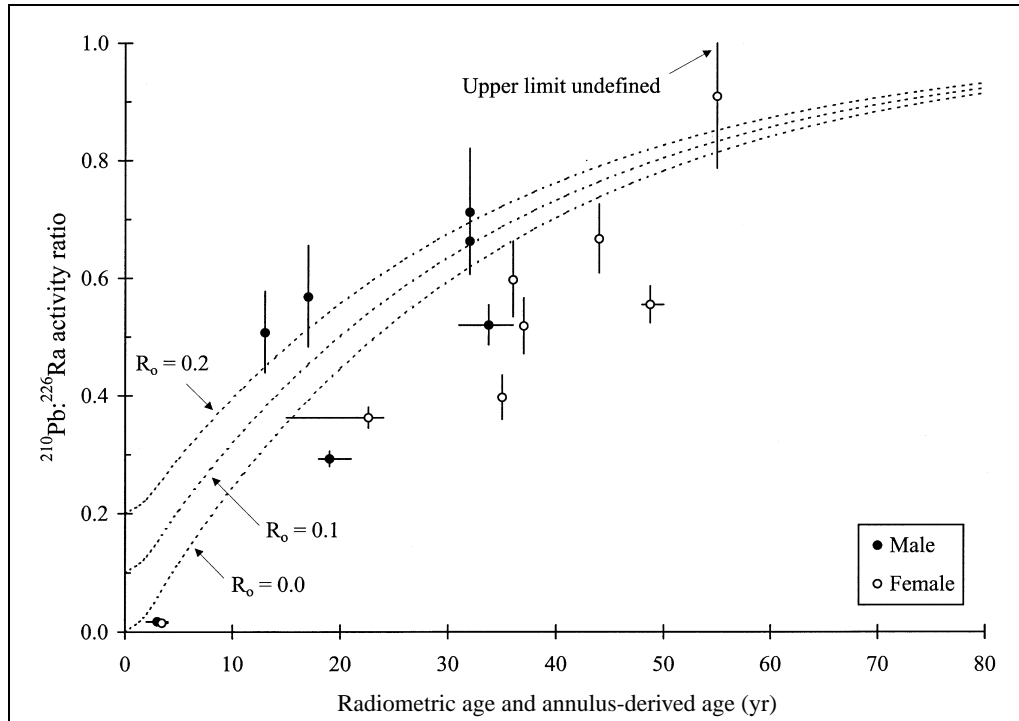


**Figure 1**

Expected  $^{210}\text{Pb}$ : $^{226}\text{Ra}$  ingrowth curves and observed  $^{210}\text{Pb}$ : $^{226}\text{Ra}$  activity ratios for male and female Atlantic tarpon (*Megalops atlanticus*) individuals and age groups. Expected ingrowth curves represent initial uptake ratios ( $R_0$ ) of 0.0, 0.1, and 0.2. Expected  $^{210}\text{Pb}$ : $^{226}\text{Ra}$  ingrowth during early otolith growth (until core-age) is based on a linear mass-growth model. After core growth, the secular equilibrium model for  $^{210}\text{Pb}$ : $^{226}\text{Ra}$  resumes and continues to unity. Data points are annulus-derived ages (average age for age groups) plotted against measured  $^{210}\text{Pb}$ : $^{226}\text{Ra}$  activity ratios. Vertical bars represent analytical uncertainty of  $^{210}\text{Pb}$  and  $^{226}\text{Ra}$  measurements. Horizontal bars represent the range of annulus-derived ages for age groups. The upper limit of the  $^{210}\text{Pb}$ : $^{226}\text{Ra}$  ratio for the oldest female exceeded 1.0; therefore, high radiometric age is mathematically undefined (Eq. 2).

**Table 3**

Comparison of annulus-derived ages and radiometric ages for *Megalops atlanticus*. The mean age of each group is based on annulus-derived age estimates. The radiometric age range is based on low and high activity ratios from analytical uncertainty calculations. The radiometric age calculations are based on the measured ratio of  $^{210}\text{Pb}$ : $^{226}\text{Ra}$ .

Age-group or single otolith age (yr)	Mean annulus-derived age (yr)	Radiometric age range (yr)	Radiometric age (yr)	Age-group or single otolith age (yr)	Mean annulus-derived age (yr)	Radiometric age range (yr)	Radiometric age (yr)
<b>Male</b>				<b>Female</b>			
2–4	3.0	1.1–1.2	1.1	3–4	3.4	0.9–1.1	1.0
13	13	19.6–28.7	23.7	15–24	22.6	14.6–16.4	15.5
17	17	22.2–35.3	28.0	35	35	15.3–19.3	17.2
18–21	19.0	11.5–12.7	12.1	36	36	25.5–35.9	30.2
31–36	33.8	22.4–27.0	24.6	37	37	21.5–27.8	24.5
32	32	31.0–56.2	41.0	44	44	31.2–42.6	36.3
32	32	31.8–40.8	35.9	48–50	48.8	24.8–29.4	27.0
				55	55	50.6–undefined <sup>1</sup>	78.0

<sup>1</sup> Upper radiometric age limit for the 78-yr female is undefined because the  $^{210}\text{Pb}$ : $^{226}\text{Ra}$  ratio exceeded 1.0.

Hence, radiometric age was determined on the basis of measured activity ratios and no adjustment for exogenous  $^{210}\text{Pb}$  was necessary. When the radiometric and annulus reading ( $\pm 12\%$  CV) age ranges were considered graphically, most of the data points still did not agree with the expected ingrowth curve ( $R_0=0.0$ ).

A direct comparison of annulus-derived age with radiometric age indicated that the ages were evenly distributed on either side of a line of agreement and that the slope of the regression (slope=0.915) was close to 1 (Fig. 2). Radiometric age was not statistically different from the annulus-derived age estimates (paired two-tailed  $t$ -test,  $df=14$ ,  $t=0.4181$ ,  $P=0.6822$ ). The coefficient of determination was low (adjusted  $r^2=0.55$ ; Kvalseth, 1985) and the power of the test to detect significant differences was low because of the variability of the data and the small sample size. The analytical uncertainty associated with radiometric age determination or the reading range of the annulus-derived age encompassed the line of agreement for only four samples. The sample with the closest agreement was a female (1780 mm FL) whose annulus-derived age was 36 years. The annulus-derived age estimates of the juvenile age groups were high by 1.9 and 2.4 years. For older age groups and individual cores, annulus-derived age was higher than radiometric age by as much as 21.8 years and

lower than radiometric age by as much as 23 years. Otolith sections that had radiometric and annulus-derived age estimates that differed considerably were photographed to illustrate the difficulty in aging otoliths (Fig. 3).

Von Bertalanffy growth functions fitted to the radiometric ages of males and females (Figs. 4 and 5) were similar to annulus-derived growth functions determined by Crabtree et al. (1995). However, the low number of radiometric data points resulted in large confidence intervals ( $\pm 95\%$ ) for growth model parameters. Radiometric-age growth parameters for males indicated an asymptotic length ( $L_\infty$ ) of  $1550 \pm 83$  mm FL and a growth coefficient ( $k$ ) of  $0.19 \pm 0.12$  (Fig. 4). Radiometric-age growth parameters for females indicated an  $L_\infty$  of  $2030 \pm 227$  mm FL and a growth coefficient ( $k$ ) of  $0.08 \pm 0.04$  (Fig. 5).

## Discussion

In four cases, the radiometric age range encompassed the annulus-derived age estimate. The oldest female tarpon had an estimate (55 yr) that was lower than the radiometric age by 23 yr. The radiometric age range, however, encompassed the annulus-derived age by 4 years. This may indicate that the annulus-derived age estimate was correct in this case. The radiometric age validation, by itself, confirms the longevity of female Atlantic tarpon to at least 50.6 yr, but it may indicate that age can meet or exceed 78.0 yr (Table 3). Similarly, the longevity of male Atlantic tarpon was confirmed to at least 31.8 yr, but may exceed 41.0 yr. When the CV for annulus-derived age was included in the range of age estimates, some additional samples encompassed the radiometric age estimates, but most deviant ages could not be explained by this variation.

The wide dispersion of residuals and the low coefficient of determination indicated that there were differences between radiometric age and annulus-derived age that could be explained in the interpretation of otolith growth zones (Fig. 2). According to Crabtree et al. (1995), aging otoliths of the Atlantic tarpon was confusing and many were not readable. Although Crabtree et al. (1995) validated the annual periodicity of growth zone formation for 12 out of 18 young fish up to an age of 9 yr in captivity, the pattern of growth zone formation in older, wild fish may not be annual. Because the tarpon is a migratory fish that inhabits inshore and estuarine waters of varying salinity and temperature and spawns offshore (Zale and Merrifield, 1989; Crabtree et al., 1992), there is a high potential for irregular growth zone formation from the stresses of extreme changes in habitat (Pannella, 1980; Campana, 1983). Subannual growth zones may explain annulus-

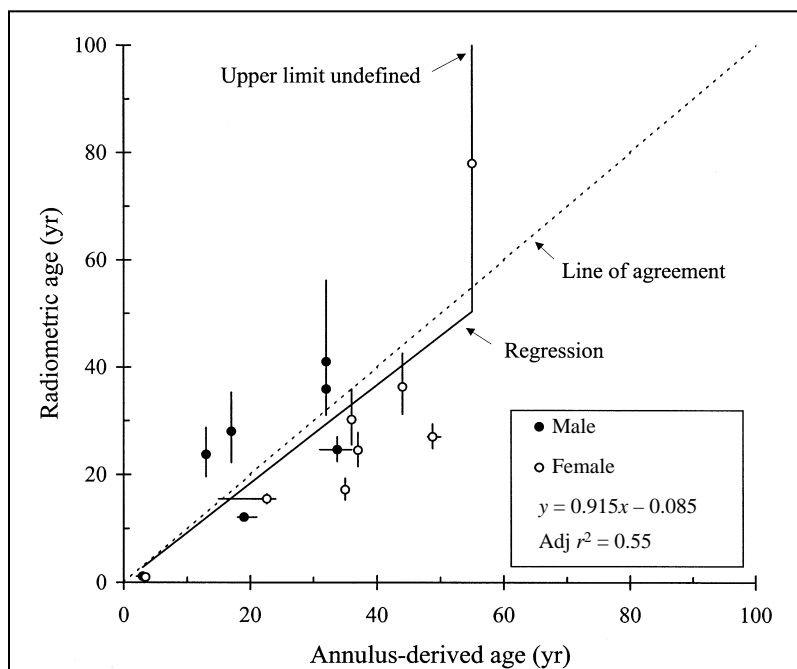


**Figure 2**

Comparison of male and female Atlantic tarpon (*Megalops atlanticus*) annulus-derived ages and radiometric ages. A linear regression and a line of agreement are plotted for comparison. Vertical bars represent low and high radiometric age estimates based on the analytical uncertainty of  $^{210}\text{Pb}$  and  $^{226}\text{Ra}$  measurements. Horizontal bars represent the range of annulus-derived ages for age groups. The upper limit of the radiometric age estimate for the oldest female is undefined because the analytical uncertainty of  $^{210}\text{Pb}$ : $^{226}\text{Ra}$  exceeds 1.0.

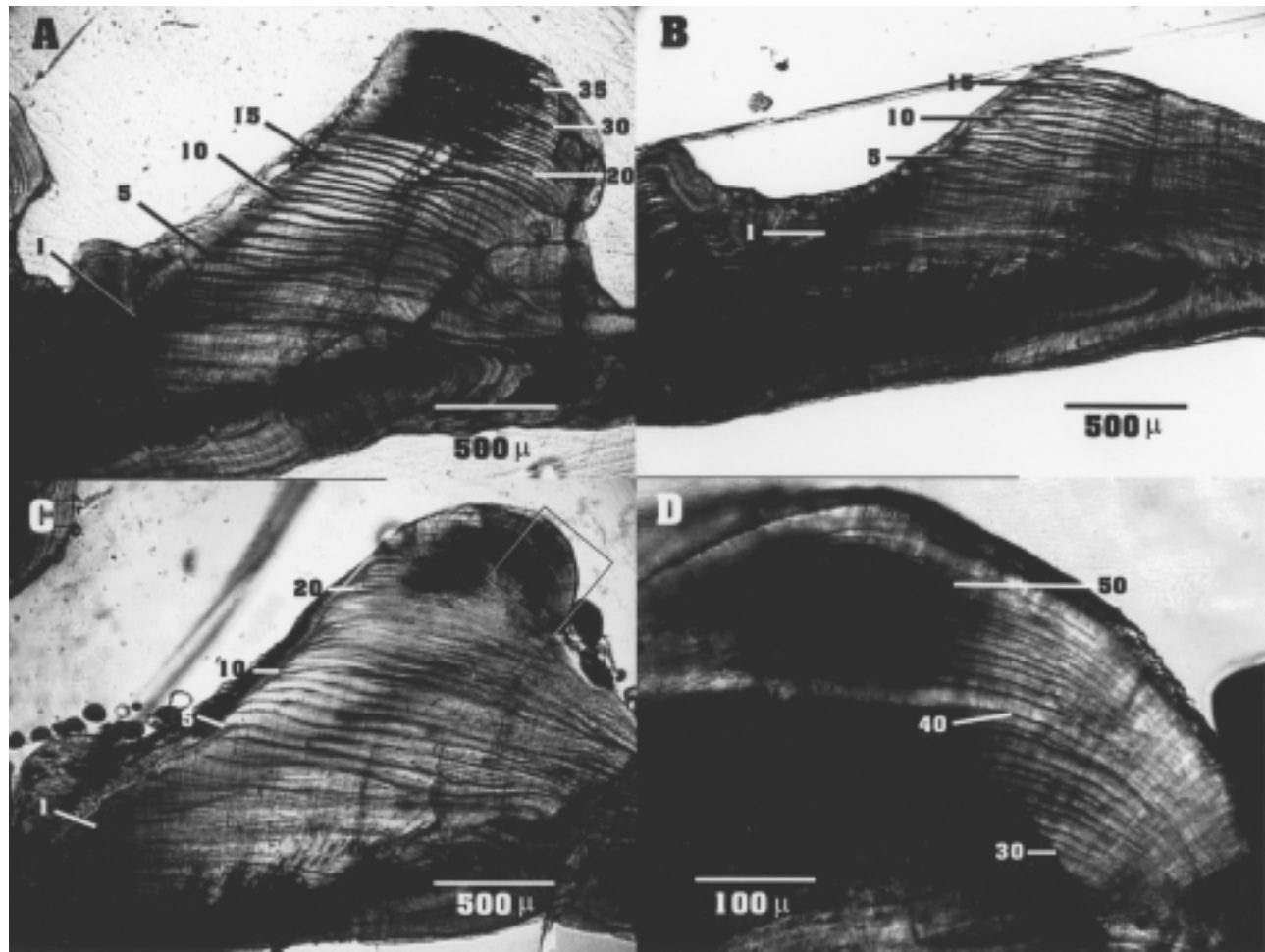


**Figure 3**

Transverse otolith sections from three Atlantic tarpon (*Megalops atlanticus*) illustrating the inherent difficulty in counting annuli. Annulus-derived ages were estimated by counting visible growth increments for each section shown (Crabtree et al. 1995). One sagitta was used for counting annuli and the other for radiometric aging. (A) An otolith section for which the number of growth increments clearly exceeds the radiometric age estimate. The annulus-derived age estimate was 37 yr and the radiometric age estimate was 24.5 yr. (B) An otolith section with fewer growth increments than the radiometric age estimate, but which could have had a higher annulus-derived age estimate if the reader had taken a more aggressive approach. The annulus-derived age estimate was 17 yr and the radiometric age estimate was 28.0 yr. (C) An otolith section with a well-developed sulcal region and numerous growth increments that rapidly become compressed toward the margin at the lower left. (D) Close up of the region in the same section (C) where growth increments are compressed and narrowly spaced. Note that growth increments in the region are partially obscured by what appears to be a proteinaceous inclusion. The annulus-derived age estimate was 55 yr and the radiometric age estimate was 78.0 yr.

derived age estimates that were higher than radiometric age. Poorly defined annual growth zones, or growth zones that become too small or compressed to be quantified, may explain annulus-derived ages that were lower than radiometric ages (Fig. 3). An additional consideration was that the age groups were composed of otoliths pooled together on the basis of annulus-derived age. This means that the radiometric age determined for these groups was the average age of the otoliths in the sample. Hence, a mixture of otoliths of differing ages would create an unac-

countable error in the radiometric age of the age groups. This variability, however, was minimized by using otoliths of similar weight.

Von Bertalanffy growth functions fitted to the radiometric ages had growth parameters that were similar to the annulus-derived growth parameters (Crabtree et al., 1995). This determination, however, is subjective because 1) there were a low number of radiometric samples, 2) the confidence intervals were large, and 3) three out of seven male samples and three out of eight female sam-

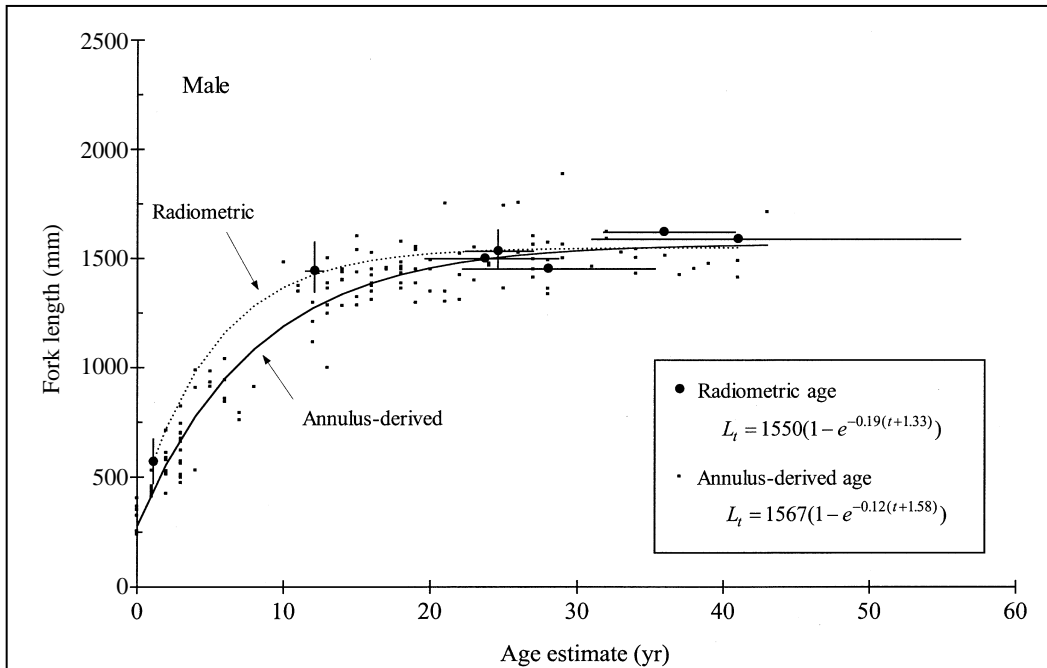


**Figure 4**

Von Bertalanffy growth curves for male Atlantic tarpon (*Megalops atlanticus*) with radiometric age (yr) and fork length (mm; average fork length for age groups) and with annulus-derived age (yr) and fork length. Vertical bars represent fork length range for age groups. Horizontal bars represent low and high radiometric age estimates.

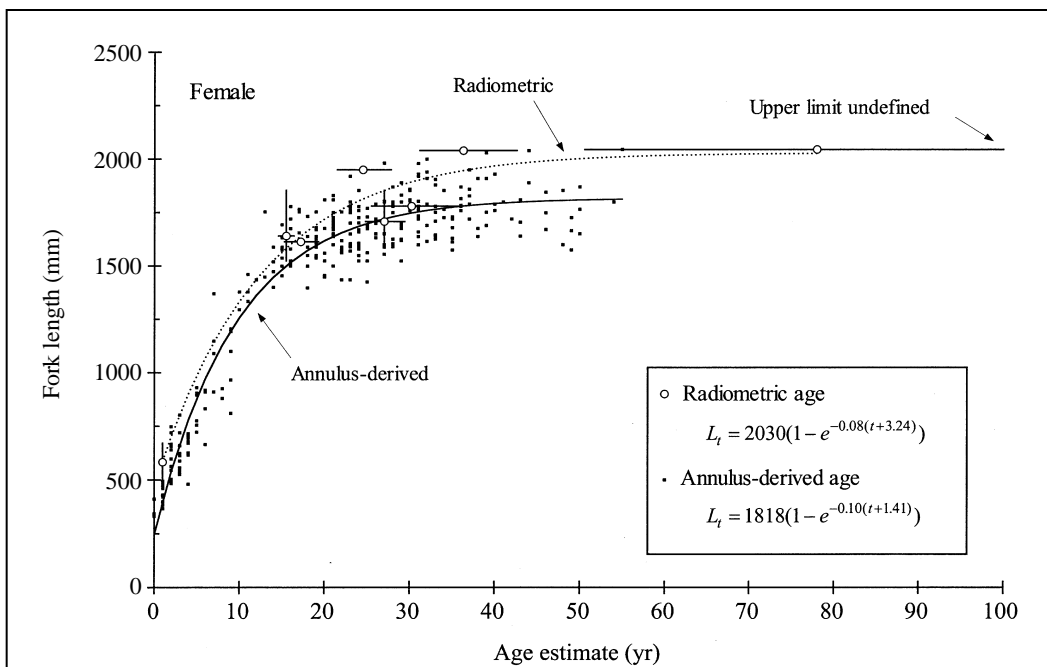


**Figure 5**

Von Bertalanffy growth curves for female Atlantic tarpon (*Megalops atlanticus*) with radiometric age (yr) and fork length (mm; average fork length for age groups) and with annulus-derived age (yr) and fork length. Vertical bars represent fork length range for age-groups. Horizontal bars represent low and high radiometric age estimates.



ples were an average age and average fork length for each age group. The growth coefficient for male radiometric ages ( $k=0.19 \pm 0.12$ ) was similar to the annulus-derived estimate ( $k=0.12$ ) according to the margin of error and was driven largely by one middle-age sample (Fig. 4). The growth coefficient for female radiometric ages ( $k=0.08 \pm 0.04$ ) was also similar to the annulus-derived estimate ( $k=0.10$ ). The male asymptotic length for radiometric ages ( $L_{\infty}=1550 \pm 83$  mm FL) encompassed the result from annulus counts ( $L_{\infty}=1567$  mm FL). For females, the asymptotic length was greater ( $L_{\infty}=2030 \pm 227$  mm FL) but still encompassed the result from annulus counts ( $L_{\infty}=1818$  mm FL). The closeness of the radiometric estimate of  $L_{\infty}$  to the maximum size was probably driven by the exceptionally large tarpon used in our study (Fig. 5).

The large size of the 2-year-old otolith core, coupled with the relatively high  $^{226}\text{Ra}$  activity and high sensitivity of the TIMS technique, permitted age determination of smaller samples than previously possible (Kastelle et al., 1994; Fenton and Short, 1995). In a recent radiometric aging study of the blue grenadier (*Macruronus novaezelandiae*), six pooled otolith cores were needed to attain a sample weight of approximately 1 g with measurable  $^{226}\text{Ra}$  activity (Fenton and Short, 1995). Although the  $^{226}\text{Ra}$  activity for the samples in that study were a factor of 10 lower than the  $^{226}\text{Ra}$  activities observed in our study, the technique used was less sensitive than TIMS and resulted in relatively high analytical uncertainties (12–21%). In a recent study of sablefish (*Anoplopoma fimbria*), where radium activities were similar to the activities observed in our study, the margin of error was relatively low (~4%), but otolith cores still needed to be pooled to attain approximately 1 g (Kastelle et al., 1994). The use of TIMS to determine  $^{226}\text{Ra}$  in our study made it possible to age age-groups that were approximately one third of a gram and individual otolith cores that were less than 0.1 g with analytical uncertainties typically less than 2%. Because of this advance, the greatest contribution to the aging error was no longer from  $^{226}\text{Ra}$  determination, but from the determination of  $^{210}\text{Pb}$  by means of  $\alpha$ -spectrometry (Andrews et al., 1999b). In our study, the determination of  $^{210}\text{Pb}$  activity contributed from 77% to 90% of the aging error.

The radiometric aging technique is well supported as a valid aging tool in numerous fish aging studies (Bergstad, 1995; Burton et al., 1999). In our study,  $^{226}\text{Ra}$  activities varied by approximately an order of magnitude, but the  $^{210}\text{Pb}$  activities never exceeded the activity of  $^{226}\text{Ra}$ . Therefore, it is highly unlikely that  $^{210}\text{Pb}$  was not the result of ingrowth from  $^{226}\text{Ra}$  incorporated during otolith formation. By performing a complete analysis on individual otoliths, we found that we could use radiometric age estimates with more confidence than estimates derived from pooled otolith samples. More recent successes with this technique (Andrews et al., 1999a) suggest that it is a reliable means to obtaining accurate age estimates. Radiometric age determinations in our study, therefore, indicate that the interpretation of growth zones in Atlantic tarpon otoliths can be difficult, and in some cases can be inaccurate. In addition, our study provides conclusive evidence that the longevity of the Atlantic tarpon is greater than 50 years.

## Conclusions

Accurate age determination of heavily harvested fish species is critical to the formulation of responsible management strategies. The typical growth-zone validation techniques have limited applicability to long-lived fishes (Mace et al., 1990; McFarlane and Beamish 1995). Underestimated longevity and overfishing were factors that led to the decline of the Pacific ocean perch (*Sebastes alutus*) and the orange roughy (*Hoplostethus atlanticus*; Beamish, 1979; Smith et al., 1995). Because of the highly variable growth zone patterns (Fig. 3) and irregular life history of the Atlantic tarpon, conventional aging methods appear to be problematic for this species. The improved radiometric aging technique used in our study incorporated a growth-zone independent chronometer that, when judiciously applied, will enable accurate age determination of many threatened species. At a time when many fish species are suffering from fishing pressure and changing oceanographic conditions, new methods need to be applied to help ascertain appropriate management strategies. The radiometric aging technique, which has been successfully applied to the sablefish, whose longevity has been validated with other techniques (Kastelle et al., 1994; Beamish and McFarlane 2000), promises to be a valuable tool for aging species with unknown or difficult-to-interpret otolith growth patterns.

## Acknowledgments

This work was supported in part by funding from the Department of the Interior, U.S. Fish and Wildlife Service, Federal Aid for Sportfish Restoration, project number F-59. Measurement of radium samples with TIMS was performed by colleagues in the Department of Earth Sciences at University of California, Santa Cruz. We especially thank Craig Lundstrom, Zenon Palacz, and Pete Holden, and the University of California, Santa Cruz. This work was presented at the First International Tarpon Symposium held at the University of Texas Marine Science Institute in Port Aransas, Texas, 15–16 February 2001. We also thank Joan Holt and the organizers of the symposium, including Paul Swacina of Tarpon Tomorrow, a nonprofit organization aimed at tarpon restoration and conservation. Additional funding was provided by a grant from the National Sea Grant College Program, National Oceanic and Atmospheric Administration, U.S. Department of Commerce, under grant number NA36RG0537, project number R/F-148 through the California State Resources Agency.

## Literature cited

- Andrews, A. H., G. M. Cailliet, and K. H. Coale.  
1999a. Age and growth of the Pacific grenadier (*Coryphaenoides acrolepis*) with age estimate validation using an improved radiometric ageing technique. *Can. J. Fish. Aquat. Sci.* 56:1339–1350.

- Andrews, A. H., K. H. Coale, J. L. Nowicki, C. Lundstrom, Z. Palacz, E. J. Burton, and G. M. Cailliet.  
1999b. Application of an ion-exchange separation technique and thermal ionization mass spectrometry to  $^{226}\text{Ra}$  determination in otoliths for radiometric age determination of long-lived fishes. *Can. J. Fish. Aquat. Sci.* 56:1329–1338.
- Beamish, R. J.  
1979. New information on the longevity of Pacific ocean perch (*Sebastes alutus*). *J. Fish. Res. Board Can.* 36:1395–1400.
- Beamish, R. J., and G. A. McFarlane.  
2000. Reevaluation of the interpretation of annuli from otoliths of a long-lived fish, *Anoplopoma fimbria*. *Fish. Res.* 46:105–111.
- Bergstad, O. A.  
1995. Age determination of deep-water fishes: experiences, status and challenges for the future. *In* Deep-water fisheries of the North Atlantic oceanic slope, NATO ASI series, series E: applied sciences, vol. 296 (A. G. Hopper, ed.), p. 267–283. Kluwer Academic Press, Netherlands.
- Burton, E. J., A. H. Andrews, K. H. Coale, and G. M. Cailliet.  
1999. Application of radiometric age determination to three long-lived fishes using  $^{210}\text{Pb}$ – $^{226}\text{Ra}$  disequilibria in calcified structures: a review. *In* Life in the slow lane: ecology and conservation of long-lived marine animals (J. A. Musick, ed.), p. 77–87. *Am. Fish. Soc. Symp.* 23, Bethesda, MD.
- Campana, S. E.  
1983. Calcium deposition and otolith check formation during periods of stress in coho salmon, *Oncorhynchus kisutch*. *Comp. Biochem. Physiol.* 75A:215–220.
- Campana, S. E., K. C. Zwanenburg, and J. N. Smith.  
1990.  $^{210}\text{Pb}$ – $^{226}\text{Ra}$  determination of longevity in redbfish. *Can. J. Fish. Aquat. Sci.* 47:163–165.
- Crabtree, R. E., E. C. Cyr, R. E. Bishop, L. M. Falkenstein, and J. M. Dean.  
1992. Age and growth of tarpon, *Megalops atlanticus*, larvae in the eastern Gulf of Mexico, with notes on relative abundance and probable spawning areas. *Environ. Biol. Fishes*, 35:361–370.
- Crabtree, R. E., E. C. Cyr, and J. M. Dean.  
1995. Age and growth of tarpon, *Megalops atlanticus*, from South Florida waters. *Fish. Bull.* 93:619–628.
- Fenton, G. E., and S. A. Short.  
1995. Radiometric analysis of blue grenadier, *Macruronus novaezelandiae*, otolith cores. *Fish. Bull.* 93:391–396.
- Flynn, W. W.  
1968. The determination of low levels of polonium-210 in environmental materials. *Anal. Chim. Acta* 43:221–227.
- Kastelle, C. R., D. K. Kimura, A. E. Nevissi, and D. R. Gunderson.  
1994. Using Pb-210/Ra-226 disequilibria for sablefish, *Anoplopoma fimbria*, age validation. *Fish. Bull.* 92:292–301.
- Kvalseth, T. O.  
1985. Cautionary note about  $R^2$ . *Am. Stat.* 39:279–285.
- Mace, P. M., J. M. Fenaughty, R. P. Coburn, and I. J. Doonan.  
1990. Growth and productivity of orange roughy (*Hoplostethus atlanticus*) on the north Chatham Rise. *N.Z. J. Mar. Freshwater Res.* 24:105–109.
- McFarlane, G. A., and R. J. Beamish.  
1995. Validation of the otolith cross-section method of age determination for sablefish (*Anoplopoma fimbria*) using oxytetracycline. *In* Recent developments in fish otolith research (D. H. Secor, J. M. Dean, and S. E. Campana, eds.), p. 319–329. The Belle W. Baruch Library in Marine Science 19, Univ. South Carolina Press, Columbia, SC.
- Pannella, G.  
1980. Growth patterns in fish sagittae. *In* Skeletal growth of aquatic organisms (D. C. Rhoades and R. A. Lutz, eds.) p. 519–560. Kluwer Academic/Plenum Publishing Corp., New York, NY.
- Saila, S. B., C. W. Recksiek, and M. H. Prager.  
1988. Basic fisheries science programs: a compendium of microcomputer programs and manual of operation. *Developments in aquaculture and fisheries science* (18). Elsevier Science Publishers, Amsterdam, 230 p.
- Smith, D. C., G. E. Fenton, S. G. Robertson, and S. A. Short.  
1995. Age determination and growth of orange roughy (*Hoplostethus atlanticus*): a comparison of annulus counts with radiometric ageing. *Can. J. Fish. Aquat. Sci.* 52:391–401.
- Smith, J. N., R. Nelson, and S. E. Campana.  
1991. The use of Pb-210/Ra-226 and Th-228/Ra-228 disequilibria in the ageing of otoliths of marine fish. *In* Radionuclides in the study of marine processes (P. J. Kershaw and D. S. Woodhead, eds.), p. 350–359. Elsevier Applied Science, New York, NY.
- Wang, C. H., D. L. Willis, and W. D. Loveland.  
1975. Radiotracer methodology in the biological, environmental, and physical sciences. Prentice Hall, Englewood Cliffs, NJ, 480 p.
- Zale, A. V., and S. G. Merrifield.  
1989. Species profiles: life histories and environmental requirements of coastal fishes and invertebrates (South Florida)—ladyfish and tarpon. *U.S. Fish Wildl. Serv. Biol. Rep.* 82(11.104). U.S. Army Corps of Engr. Report TR EL-82-4, 17 p.